Development of Adagrasib's Commercial Manufacturing Route

David Snead*, Yonghong Gan*, Thomas Scattolin, Dinesh J. Paymode, Michal M. Achmatowicz, Duane E. Rudisill, Ephraim S. Vidal, Tawfik Gharbaoui, Phil Roberts, Jianbo Yang, Zhangbing Shi, Wei Liu, Joshua Bolger, Zhen Qiao, and Cheng-yi Chen*

Adagrasib, KRAS-G12C, Oncology, Targeted Covalent Inhibitor

Abstract A commercial route to **MRTX849** (adagrasib) was developed to support clinical and commercial needs. Yield was improved to 32% over six chemical steps. A doubly regioselective S_NAr reduced consumption of an expensive chiral intermediate, reaction optimization led to parts per million palladium catalysis, and a new method to deprotect Cbz-groups were developed to mitigate risk associated with benzyl iodide.

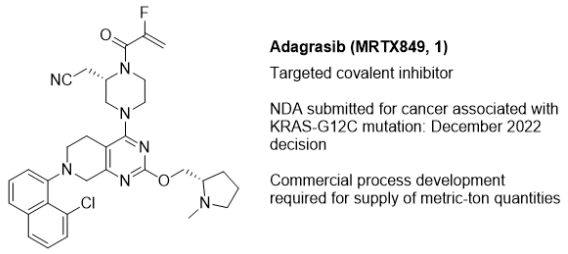

Figure 1: Adagrasib.

■ Introduction and Assessment of Reported Route:

Kirsten rat sarcoma (KRAS) is the most frequently mutated oncogene and is associated with several highly fatal cancers.[1] Exceptional recent advances have resulted in drug candidates for this target which was once considered undruggable. Adagrasib (**MRTX849**, **1**, Figure 1) is a therapy for treatment of non-small cell lung cancer which results from G12C point mutation to the KRAS gene.[2] The NDA filing for this drug candidate is under FDA review with a decision to be made in December, 2022. Supporting further clinical combination trials and commercial manufacture for sizable patient populations requires ability to consistently produce ton scale quantities with a high degree of control. This publication communicates those efforts.

Commercial route development began with review and analysis of adagrasib's reported route (Figure 2).[3] Iterative side-chain appendage to bicyclic pyrimidine core **2** resulted in a modular and convergent synthesis, and reparation required a longest linear sequence (LLS) of 8 synthetic step from available building blocks.

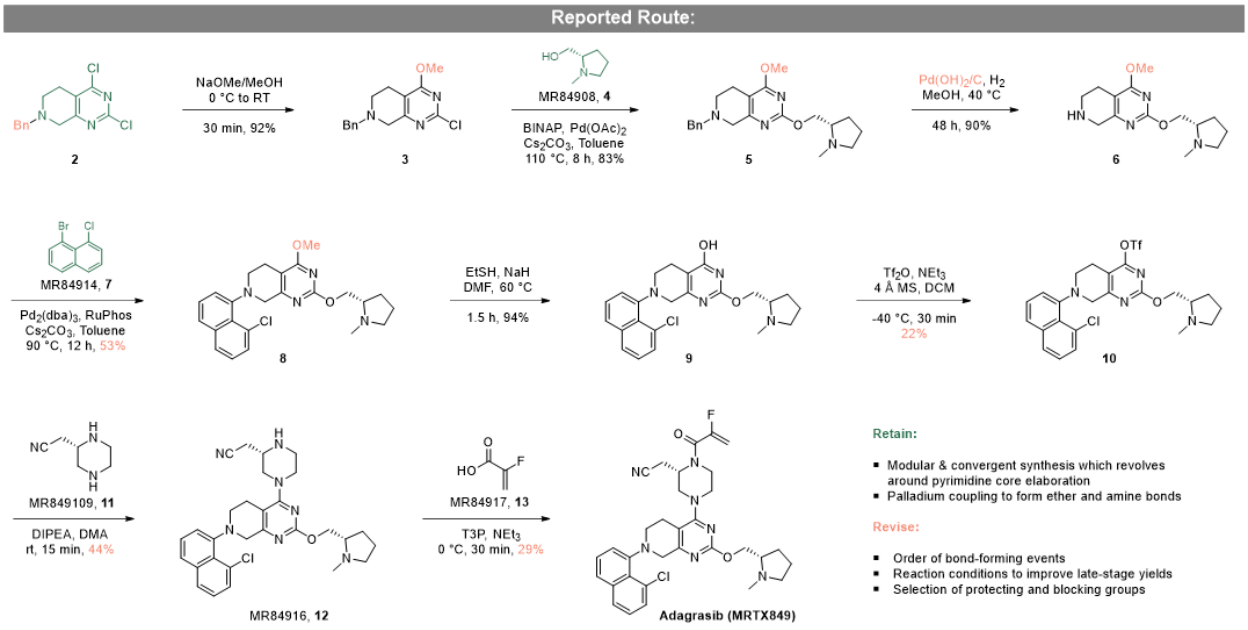

Figure 2: Reported route to adagrasib, highlighting features to retain and revise.

Synthesis commenced by forming a methanol adduct of **2** at the northern aryl chloride's position. Blocking this site preserved S_NAr reactivity at a later point in the synthesis and allowed regioselective prolinol attachment at the

southeastern aryl chloride's location forming **5**. Palladium hydroxide debenzylation and the ensuing Buchwald-Hartwig amination enabled the subsequent naphthyl chloride installation (**8**). Only piperazine appendage remained with two of the three side-chains affixed. This however necessitates demethylation and activation of the previously installed ether, adding to the LLS. Once this is done, chiral piperazine **11** can be connected to the pyrimidine ring via a S_NAr reaction. This nucleophilic attack shows intriguing regioselectivity despite addition as the naked diamine and modest yield. Reaction with 2-fluoroacrylic acid (**13**) completed the synthesis without exposing the sensitive acrylamide warhead to multiple synthetic operations.

The low overall yield (1%) clearly must be addressed in order to support early clinical studies and supply the market. This was largest challenge and arose from a series of low yielding steps tied to installation of the chiral piperazine and acrylamide. Reducing the LLS step-count would also further streamline and debottleneck production.

We imagined achieving these goals *via* a reordered sequence of bond-forming events which harness the pyrimidine's natural reactivity (Figure 3). Introducing the piperazine early could be particularly beneficial. The northern aryl chloride presents itself as the pyrimidine's most reactive electrophile. Conducting the S_NAr in this way eliminates 3 steps related to protection, demethylation, and activation at this locus. Moreover, a high-yielding transformation would resolve two particularly low-yielding operations. The synthesis would then revert to the established sequence of bond forming events (etherification → arylation → acylation).

Three starting material structures' were tweaked to enhance production. The piperidine was protected with *tert*-butoxy carbamate (Boc) rather than benzyl group, the piperazine was differentially protected as a benzyl carbamate (Cbz) adjacent to the methyl cyanide, and the sodium salt of fluoroacrylic acid replaced the acid. Boc-protection of piperidine was desired to remove the need for expensive palladium in a simple deprotection, Cbz-protection was chosen for the piperazine to nullify compatibility issues in the downstream Buchwald-Hartwig coupling, and the sodium salt was selected for improved reactivity in the amide formation.

■ Commercial Route Development

Step 1:

Investigation of reactivity between pyrimidine **14** (**MR84906**) and chiral piperazine **15** (**MR84905**) kicked-off the new route's exploration. The reaction worked excellently, in parallel to the high-yielding formation of the methanol adduct. Product was isolated in 90% yield after crystallization. Byproducts associated with incorrect regiochemical addition (**18**) and unmasking of free piperidine (**19**) were held to less than 1% each and most often, less than 0.2%.

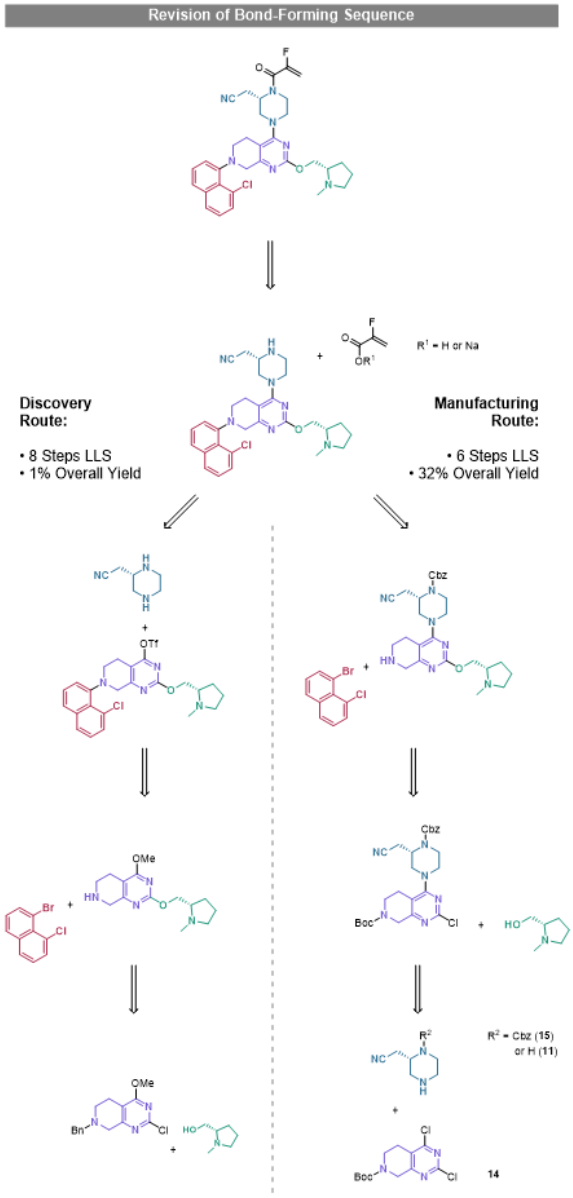

Figure 3: Comparison of routes to adagrasib.

Even more strikingly, free-piperazine (**MR849109**, **11**) successfully reacted with **14**, without impurities related to nucleophilic attack by the undesired amine (**20**). Neither amine nor pyrimidine reactive sites required protection. The amine could then be capped with a Cbz group *in situ* to intercept the same intermediate as Route 1, **MR84907**. Ability to use free diamine is particularly important since its synthetic preparation is much shorter than that of the

protected piperazine,[4] and its molecular weight is half that of the Cbz protected fumarate salt thus reducing consumption of this expensive ingredient (Figure 5). This provides an option which significantly reduces cost.

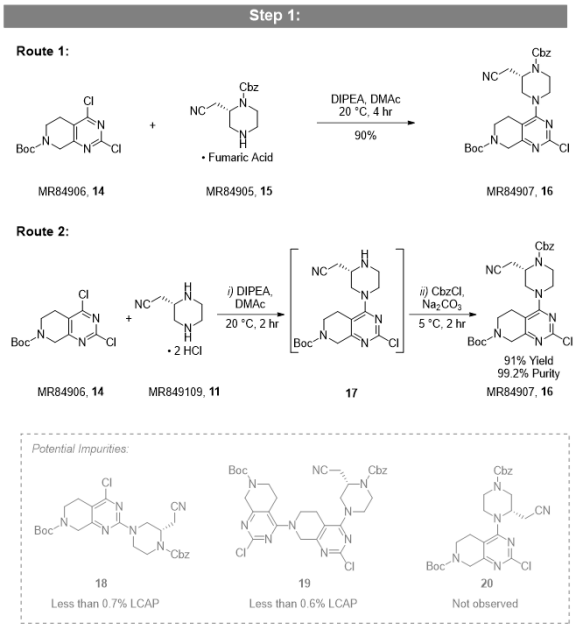

Figure 4: Synthesis of **MR84907** (**16**) from protected or free piperazine.

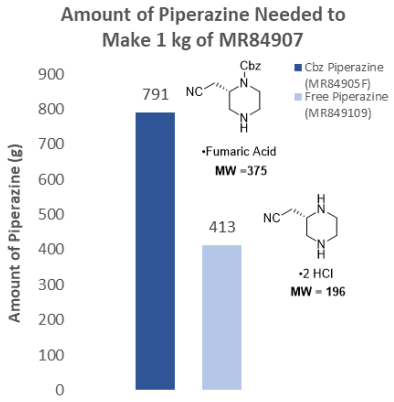

Figure 5: Consumption of piperazine based on **MR84907** Routes 1 and 2.

Successful high-yielding installation of the piperazine represented a major program accomplishment. This resolved the low yield associated with the hydroxyl activation and ensuing S_NAr (9.7% yield over two steps). It also negated multiple operations related to use of an ether protection group.

Step 2&3:

The palladium catalyzed C—O bond formation proceeded quite well by the initial medicinal chemistry development. Even so, several items still required additional refinement.

Firstly, the reaction needed to be more robust. Occasionally the rate decelerated, and then the reaction stalled. Secondly, cesium carbonate is moderately expensive and its high molecular weight results in large quantities consumed. Lastly, palladium pricing is quite high (up to $100,000/kg) so reduction of the original 10 mol% $Pd(OAc)_2$ loading is essential. The $Pd(OH)_2/C$ deprotection was eliminated by using the Boc-protected piperazine **MR84907** which was easily deprotected with HCl.

Investigation revealed that residual formaldehyde could be present in the coupling partner, prolinol (**MR84908**). Setting tight control on formaldehyde greatly improved the catalyst activity. When present at 1.5% by weight, the reaction required 88 hr to reach completion. Moreover, the in process HPLC analysis showed low purity of the intermediate and substantial generation of an impurity resulting from hydrolysis of the aryl chloride (~10% a/a). At 0.2% formaldehyde however, **MR84907** reacted fully within 15 hr (0.6% residual **MR84907**).

To further improve the system the reaction was run in 2-MeTHF, $Pd_2(dba)_3$ replaced $Pd(OAc)_2$, and K_3PO_4 was chosen as the base instead of Cs_2CO_3. Combining these benefits allowed catalyst loading to be reduced to 1.5 mol% (Figure 6).

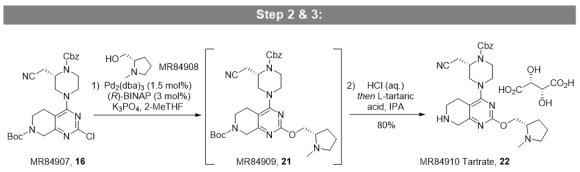

Figure 6: Commercial route to **MR84910** Tartrate.

Still, given the expense of palladium an option to further minimize consumption was desired. Subsequent screening identified Xantphos as a ligand imparting high catalyst activity. 0.25-0.5 mol% catalyst loading effectively promoted the reaction, thus essentially rendering the cost of palladium in this step negligible (Figure 7).

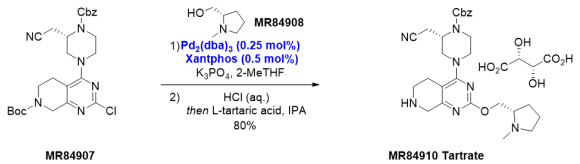

Figure 7: Xantphos enables ppm level palladium loading.

Unfortunately, the reaction showed sensitivity to scaling at these levels, and the initial results obtained at small scale did not reproduce when performed in jacketed vessels with overhead stirrers. Reaction kinetics revealed strong dependence on concentration of potassium phosphate and prolinol,[5] suggesting that formation of a transmetallating agent might be rate limiting. Microscopy showed that the phosphate surface area was greatly increased by grinding action of the stir-bar. Comparing commercial phosphate with ground phosphate showed the high-surface area phosphate was considerably more active. Reactions were run on a heated shaker block to eliminate mixing and grinding effects (Figure 8). Wet-milling the hygroscopic phosphate in 2-MeTHF similarly increased reaction rate and provided a kilogram scale approach to reproduce this effect and enhance reaction kinetics at low catalyst loading (Figure 9).

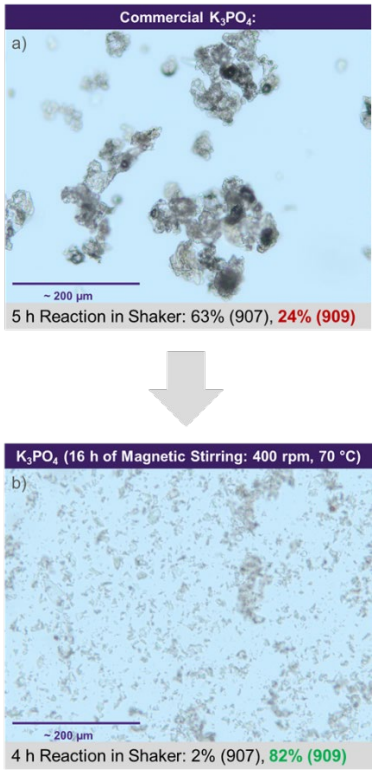

Figure 8: a) Coupling of **MR84907** and **MR84908** with commercial potassium phosphate. b) Coupling of **MR84907** and **MR84908** with potassium phosphate ground by a magnetic stir-bar. Reactions run with 0.5 mol% $Pd_2(dba)_3$ and 1.0 mol% Xantphos.

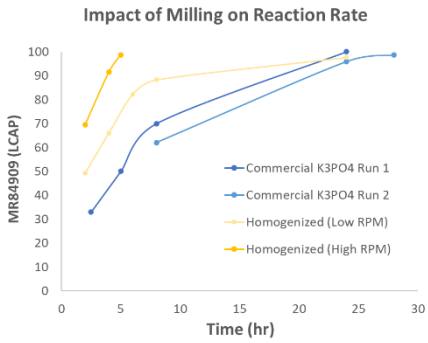

Figure 9: Comparison of **MR84907** and **MR84908** coupling reactions run in overhead stirrer with or without homogenization (wet-milling). Reactions run with 0.5 mol% $Pd_2(dba)_3$ and 1.0 mol% Xantphos.

Step 4:

The initial development made use of a $Pd_2(dba)_3$/RuPhos catalyst system. With Cs_2CO_3 **MR84915** was obtained in moderate yield with improvement desired. RuPhos, Cs_2CO_3 and toluene were replaced with (*R*)-BINAP, K_3PO_4, and 2-MeTHF. Again, wet-milling the phosphate improved robustness. These modifications substantially increased the assay yield. The installation of naphthylamine proceeded cleanly, but with only modest to good efficiency (80-90% assay yield, Figure 10). The kinetic studies showed that productive and product decomposition pathways are competing with the latter becoming more dominant at high conversions (>90% of **MR84910**, Figure 11). To prevent **MR84915** assay loss the stirout time had to be limited to less than 30 hr. **MR84915** product resisted crystallization as a freebase and amorphous precipitations (e.g. 2-MeTHF-heptane) offered little in a way of impurity control resulting in **MR84915** of suboptimal quality (~93% LC, 300 ppm Pd). While the salt screening identified only one crystalline hit – **MR84915**-*p*-toluenesulfonate – it satisfied the criteria of developability (robust crystallinity, thermal stability up to 140 °C, 1:1 stoichiometry, solubility profile, impurity rejection). Exploration of suitable crystallization solvents eventually led to 2-MeTHF-acetone mixtures which provided excellent impurity rejection, acceptable recovery, with minimal processing complexity. Finding optimal 2-MeTHF-acetone ratio (50:50 v/v) required balancing recovery (better at higher 2-MeTHF) and good crystallization kinetics (better at lower 2-MeTHF). In addition, ensuring the ratio of *p*-TSA to freebase (FB) is sightly below unity was critical for the optimal conversion and recovery as the solubility of **MR84915**-*p*-TSA salt curves up right past the equivalency point (Figure 12).

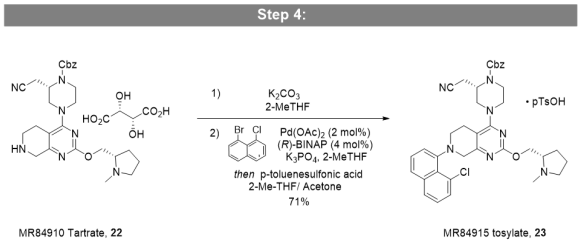

Figure 10: Commercial route to **MR84915** Tosylate.

By recrystallizing the intermediate with 0.98 equivalents of *p*-TSA 71% of **MR84915** salt could be isolated, a 20% improvement from the early development.

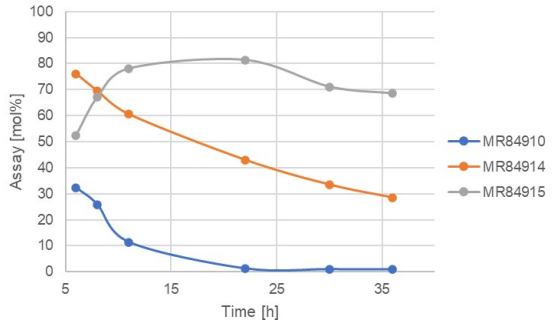

Figure 11: Kinetic profile of Buchwald-Hartwig amination (Step 4) showing competitive decompostion of **MR84915** product.

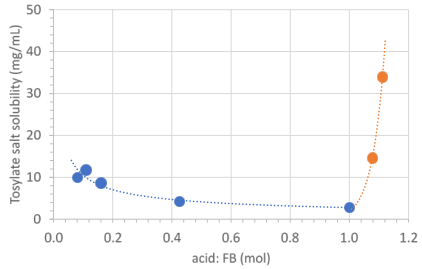

Figure 12: Solubility profile of **MR84915** Tosylate salt vs. acid/FB molar ratio in 50:50 (v/v) 2-MeTHF/acetone.

Step 5:

Cbz piperazine protection imparts differential reactivity between the carbamates of **MR84907**; however an additional step is required to reveal the piperazine's free amine. Trimethylsilyl iodide (TMSI) is a traditional deprotection reagent for this transformation.[6,7] A number of batches were made using this methodology; however, benzyl iodide (BnI), a potentially mutagenic impurity (PMI) is coproduced. Though it purges well, elimination of this hazard is desired. Additionally, BnI can be trapped by the basic site (tertiary amine) of the prolinol generating a quaternary ammonium species. The removal of this species is not trivial and required the use of silica plug at the API stage in order to be fully rejected.

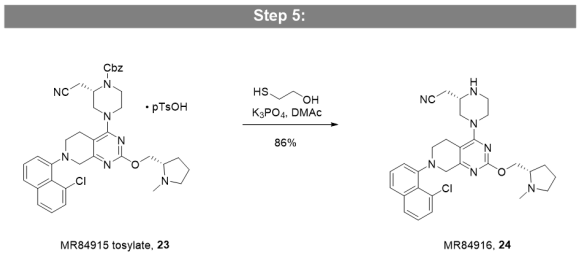

Figure 13: Commercial route to **MR84916**.

A new Cbz-deprotection was developed which avoids BnI production.[8] Reaction of **MR84915** Tosylate with 2-mercaptoethanol cleanly released the benzyl group and carbon dioxide. The coproduct of reaction (thioether) is a benign liquid which easily purges, and the thiol precursor is surprisingly minimally odiferous.[9] By running the reaction in *N,N*-dimethylacetamide (DMAc) with K_3PO_4, there was no need to first isolate the free base of the acid complex, and **MR84916** could be crystallized directly from the reaction mixture using water thus minimizing consumption of organic solvents (Figure 13).[10]

Epimerization of the cyanomethyl was an unexpected consequence of the reaction under basic conditions. Conducting Step 5 without 2-mercaptoethanol illustrates this concept, and the epimer content increases over time (Figure 14). The protons alpha to the nitrile can be deprotonated prior to deprotection of the carbamate. This species is then prone to piperazine ring opening via formation of an acrylonitrile. Subsequent Michael addition leads to the epimerization as the carbamate can attack either face of the olefin. Analogous experiments show that the deprotected **MR84916** is not prone to epimerization since the amine is a poor leaving group.

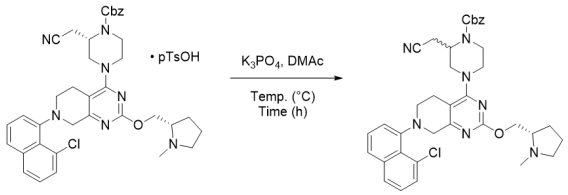

epi-MR84915 (%)	25 °C	40 °C	75 °C
2 h	0.22%	0.6%	28.77%
16 h	0.22%	20.78%	49.92%

Figure 14: Epimerization of piperazine under basic conditions in the absence of 2-mercaptoethanol.

Table 1: 3-Factor, 2-Level Design of Experiments to understand factors impacting epimerization of chiral piperazine. Input material contains 0.22% of ***epi*-MR84915.**

K_3PO_4 (equiv.)	Temp (°C)	Water Content (ppm)	*epi*-MR84916 (%)
3.5	65	200	0.99%
3.5	65	2000	0.48%
3.5	85	200	1.30%
3.5	85	2000	1.30%
4.5	65	200	0.54%
4.5	65	2000	1.10%
4.5	85	200	0.96%
4.5	85	2000	1.50%

Characterization of the reaction *via* design-of-experiments (DoE) helped determine factors which impacted the reaction and define a robust operational space. Epimerization depends primarily upon temperature and water content, where higher values of these factors increased formation of the diastereomer. The reaction was well controlled by setting appropriate limits on these variables, and the diastereomer could be tolerated at levels up to 4% since ~50% purges in each of the two crystallization steps of **MRTX849**.

Step 6:

Installation of the acrylamide warhead was low-yielding in the initial developments. Minor refinements lead to substantial gains, however (Figure 15). Use of the sodium salt of 2-fluoroacrylic acid promoted both acylation activity and stability of the starting material and eliminated need for external base (Et_3N). This greatly improved yield to 89% AY and 70% IY. The majority of material loss occurred during two crystallizations which were conducted to ensure exceptional purity of the final API.

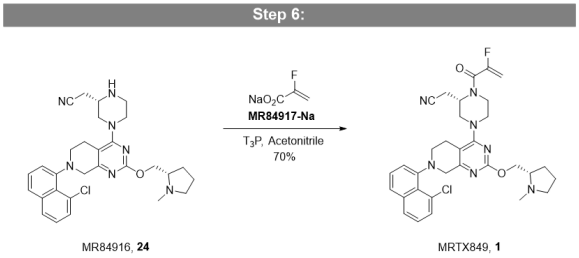

Figure 15: Coupling **MR84916** and **MR84917-Na** to produce API, **MRTX849**.

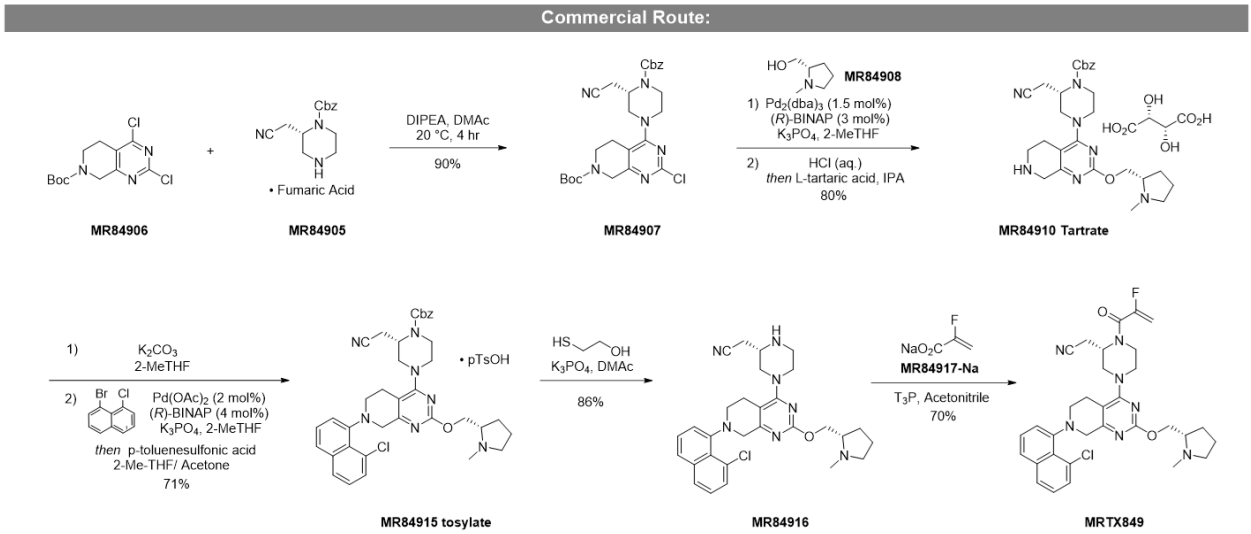

Figure 16: Synthetic route for production of **MRTX849** (adagrasib).

■ **Conclusions:**

Changing the sequence of bond-forming events led to a robust and scalable production route for **MRTX849**. Yield of API increased to 32% while reducing the sequence to six GMP steps (Figure 16). Intermediate production was conducted at scales of up to 300 kg with 100 kg batches of final API, and metric-ton quantities were made to supply clinical and commercial needs. A doubly regioselective S_NAr provides the option to reduce consumption of an expensive chiral intermediate, reaction optimization led to parts per million palladium catalysis, and a new method to deprotect Cbz-groups was developed to mitigate the risks associated with benzyl iodide generated under conventional TMSI deprotection strategy.

Acknowledgements

Our valued collaborators helped make this project real, and Mirati is very grateful for their many contributions. Neil

Andersen provided guidance on process development and Patricia Andres provided insight into the final crystallizations. Yibin Lin, Runkai Li, and Elise Bradley provided analytical support. Sharon Real and Elli Chatzopoulou's input guided our regulatory strategy. Asymchem's expertise was essential for quickly implementing API manufacture. We are very thankful that Porton and Bellen provided quality building blocks for the project. TCG Lifesciences, Hangzhou Allsino, and Innosynn provided impactful proof-of-concept work on MR849109, MR84907, and MR84910 respectively.

Associated Content:

Supporting information including procedures and compound characterization available free of charge.

Author Information:

Corresponding Author Information:

David Snead: sneadd@mirati.com
Yonghong Gan: gany@mirati.com
Cheng-yi Chen: chenc@mirati.com

Authors:

David Snead: Mirati Therapeutics, Inc. 3545 Cray Ct, San Diego, CA 92121
Yonghong Gan: Mirati Therapeutics, Inc. 3545 Cray Ct, San Diego, CA 92121
Thomas Scattolin: Mirati Therapeutics, Inc. 3545 Cray Ct, San Diego, CA 92121
Dinesh J. Paymode: Mirati Therapeutics, Inc. 3545 Cray Ct, San Diego, CA 92121
Michal Achmatowicz: Mirati Therapeutics, Inc. 3545 Cray Ct, San Diego, CA 92121
Duane Rudisill: Mirati Therapeutics, Inc. 3545 Cray Ct, San Diego, CA 92121
Ephraim Vidal: Mirati Therapeutics, Inc. 3545 Cray Ct, San Diego, CA 92121
Tawfik Gharboui: Mirati Therapeutics, Inc. 3545 Cray Ct, San Diego, CA 92121
Phil Roberts: Mirati Therapeutics, Inc. 3545 Cray Ct, San Diego, CA 92121
Jianbo Yang: Asymchem Life Science (Tianjin) Co., Ltd., No. 71, 7th Avenue, TEDA Tianjin, 300457, P.R. China
Zhangbing Shi: Asymchem Life Science (Tianjin) Co., Ltd., No. 71, 7th Avenue, TEDA Tianjin, 300457, P.R. China
Wei Liu: Asymchem Life Science (Tianjin) Co., Ltd., No. 71, 7th Avenue, TEDA Tianjin, 300457, P.R. China
Joshua Bolger: Asymchem, Inc., 600 Airport Blvd. Suite 1000, Morrisville, NC 27560
Zhen Qiao: Asymchem Life Science (Tianjin) Co., Ltd., No. 71, 7th Avenue, TEDA Tianjin, 300457, P.R. China
Cheng-yi Chen: Mirati Therapeutics, Inc. 3545 Cray Ct, San Diego, CA 92121

■ **Experimentals:**

MR84907 (16): The manufacturing process begins by charging *N*,*N*-Dimethylacetamide (DMAc) (708 kg, 3.54 X [X is weight to weight ratio (w/w) to the basis charge]) to an inerted reaction vessel. After ensuring that the water content is not more than 0.1%, MR84905F is added (260 kg, 1.30 X, 1.05 equiv.). Agitation is turned on, and the mixture is adjusted to a temperature of 10-20 °C. *N*,*N*-Diisopropylethylamine (DIPEA) is then added (170 kg, 0.85 X, 2.00 equiv.), followed by the charge of MR84906 (200 kg, 1.00 X, 1.00 equiv.) while maintaining the temperature range. The mixture is allowed to react for not less than 2 hours and then tested for completion by HPLC. The reaction is judged to be finished when there is not more than 1.0% a/a of MR84906 remaining. After obtaining a passing IPC, methyl *tert*-butyl ether (MTBE) is charged (1480 kg, 7.40 X) at a temperature between 10-30 °C. The mixture is then heated to 30-40 °C, and water is added (1000 kg, 5.00 X) at a rate which allows the temperature of the mixture to be maintained. The aqueous layer is separated and discarded. The MTBE fraction is then washed with an aqueous mixture of sodium chloride and concentrated under reduced pressure. MR84907 seed is added (0.6 kg, 0.003 X) at a temperature of 30-40 °C, aged, and then *n*-Heptane anti-solvent is added. The suspension is cooled to 15-25 °C and aged further to complete the crystallization. The solids are collected by filtration, rinsed with *n*-heptane, and dried until the sum of MTBE and *n*-heptane are not more than 2.0% and water content is not more than 1.0%. 324 kg of off white solid was collected with 95.4 wt% potency and 98.5% area to area (a/a) purity (90% yield).

^{1}H NMR (400 MHz, $CDCl_3$) δ 7.49 – 7.31 (m, 5H), 5.36 – 5.11 (m, 2H), 4.77 – 4.57 (m, 2H), 4.44 (d, J = 19.4 Hz, 1H), 4.06 (m, 2H), 3.85 (m, 2H), 3.38 (m, 3H), 3.11 (td, J = 12.4, 3.5 Hz, 1H), 2.95 – 2.54 (m, 4H), 1.49 (s, 9H) ppm. **^{13}C NMR** (101 MHz, $CDCl_3$) δ 165, 157.67, 154.81, 154.20, 135.79, 128.67, 128.49, 128.36, 117.01, 113.90, 80.67, 68.11, 48.36, 47.71, 41.15, 39.75, 39.28, 28.38, 26.23, 19.24 ppm. **HRMS** (ESI) calculated for $C_{26}H_{32}ClN_6O_4$: 527.2174 $[M+H]^+$, Found: 527.2283.

MR84910 Tartrate (22): Step 2: Charge 2-MeTHF (2562 kg, 8.54 X) to a suitable inert reaction vessel and test to ensure water content is not more than 0.5%, followed by charge MR84907 (300 kg, 1.00 X, 1.00 equiv.). The resulting mixture is stirred at 10–30°C to provide a homogeneous solution and to the vessel is then charged anhydrous K_3PO_4 (363 kg, 1.21 X, 3.00 equiv.) and regulatory starting material MR84908 (99.0 kg, 0.33 X, 1.50 equiv.). The mixture is degassed and to the vessel is then charged (*R*)-BINAP (10.5

kg, 0.035 X, 0.030 equiv.) and $Pd_2(dba)_3$ (7.80 kg, 0.026 X, 0.015 equiv.). The reaction mass is heated to a temperature range of 77–80°C for not less than 20 hours and subsequently sampled for HPLC analysis to determine reaction completeness. The reaction is deemed to be complete when the level of residual MR84907 relative to product MR84909 is not more than 3.0% a/a. Upon achieving a conforming IPC result the mixture is cooled to 15–38°C and to the vessel is then charged purified water (1500 kg, 5.00 X). The aqueous phase is then separated and discarded. The organic phase is washed with aqueous NaCl (5.21 wt%, 633 kg, 2.11 X). The aqueous phase is separated and discarded and the organic process stream containing MR84909 is telescoped into the next process operation.

In Step 3 of the manufacturing process, the MR84909 solution is acidified with hydrochloric acid solution (9.33 wt%, 1610 kg, 5.35X, 7.00 equiv.) and the resulting aqueous phase containing the MR84909 hydrochloride salt is held at 15-25°C to affect a Boc-deprotection reaction. The mixture is sampled for HPLC analysis to determine the level of residual MR84909 (acceptance criterion not more than 1.0% a/a). Upon achieving a passing IPC result, the mixture is extracted with 2-MeTHF (513 kg, 1.71 X) and the organic phase is separated and discarded. The resulting aqueous phase is adjusted to approximately pH 9 by addition of potassium carbonate solution (30.0 wt%, 1840 kg, 6.12 X). To the basic aqueous phase is added sodium chloride (480 kg, 1.6 X) and the resulting phase is extracted with 2-MeTHF (2560 kg, 8.54 X then 1280 kg, 4.27 X). The combined organic extracts are then concentrated under reduced pressure. Azeotropic distillation is then performed with additional 2-MeTHF (1030 kg, 3.42 X) until the water content is not more than 0.5% w/w as measured by Karl Fischer analysis. After charcoal treatment, the resulting solution is heated to approximately 45-55 °C and treated with a solution of *L*-tartaric acid (84.0 kg, 0.28 X, 1.00 equiv.) in IPA (942 kg, 3.14 X). The reaction mass is cooled to 20–30°C causing intermediate MR84910 Tartrate salt to crystallize. The solids are then isolated by filtration, washed with successive portions of 2-MeTHF (63 kg, 0.21 X) and dried. 326 kg of white solid was obtained with 70.75 wt% assay as the free base and 95.9% a/a purity (80% yield).

^{1}H NMR (400 MHz, DMSO-d_6): δ 7.41 – 7.33 (m, 5H), 5.18 – 5.08 (m, 2H), 4.62 – 4.57 (m, 1H), 4.28 (dd, J = 11.1, 5.6 Hz, 1H), 4.16 (dd, J = 11.1, 5.6 Hz, 1H), 4.00 – 3.98 (m, 3H), 3.96 – 3.92 (m, 2H), 3.91 – 3.76 (m, 2H), 3.42 – 3.23 (m, 1H), 3.18 – 2.99 (m, 5H), 2.96 – 2.87 (m, 2H), 2.85 – 2.79 (m, 1H), 2.73 – 2.67 (m, 2H), 2.47 (s, 3H), 2.40 (q, J = 8.7 Hz, 1H), 2.03 – 1.93 (m, 1H), 1.77 – 1.68 (m, 2H), 1.66 – 1.60 (m, 1H) ppm. **^{13}C NMR** (101 MHz, DMSO-d_6): δ 174.9 (2C), 166.5, 162.3, 162.1, 154.8, 136.9, 128.9 (3C), 128.4, 128.1, 119.0, 109.0, 72.3 (2C), 68.2, 67.3, 64.5, 57.2 (2C), 49.0, 47.7, 47.5, 41.8, 41.3 (2C), 28.4, 23.8, 22.8 (2C) ppm. **HRMS** (ESI) calculated for $C_{27}H_{36}N_7O_3$: 506.2880 $[M+H]^+$, Found: 506.3000.

MR84915 Tosylate (23): The synthesis commences by charging an inert reaction vessel with MR84910 Tartrate (230 kg, 1.00 X), purified water (920 kg, 4.00 X), followed by 2-MeTHF (2374 kg, 10.3 X). The resulting mixture is then treated with an aqueous solution of K_2CO_3 (30.0 wt%) to adjust the pH to within the range of approximately 8–9. To the vessel is then charged sodium chloride (230 kg, 1.00 X) and the reaction mass is then stirred at 20-35°C. The layers are separated, and the resulting organic phase is washed with brine solution (20 wt%, 575 kg, 2.5 X). Azeotropic distillation is then performed with additional 2-MeTHF (593 kg, 2.58 X) until the water content is not more than 0.5% w/w as measured by Karl Fischer analysis.

To a second inert reaction vessel is charged anhydrous K_3PO_4 (386 kg, 4.00 equiv.) and 2-MeTHF (989 kg, 4.30 X). The resulting heterogenous mixture is wet-milled. The previously obtained distillation residue is filtered through charcoal and added to the milled phosphate mixture rinsing forward with additional 2-MeTHF (198 kg, 0.86 X). To the vessel is then added regulatory starting material MR84914 (120 kg, 0.52 X, 1.09 equiv.) and the mixture is degassed with nitrogen. To the vessel is added (*R*)-BINAP (11.3 kg, 0.049 X, 0.040 equiv.) and $Pd(OAc)_2$ (2.05 kg, 0.0089 X, 0.020 equiv.) under nitrogen protection and the resulting reaction mixture is heated to 75–85°C. The reaction is considered complete when residual MR84910 relative to MR84915 reaches not more than 3.0% or not more than 10.0% after reaction for 30 hours. The reaction mass is then cooled and to the vessel is charged purified water (1150 kg, 5.0 X) while maintaining a batch temperature of 20–30°C. The phases are separated and the organic stream is washed with brine (13.0 wt%, 1320 kg, 5.75 X) followed by extraction with a aqueous mixture of citric acid (according to residual MR84910 content) and sodium chloride (13.0 wt%, 794 kg, 3.45 X). The organic layer is separated and assayed by HPLC to ensure the level of residual MR84910 is not more than 0.5% a/a. In the event of a non-conforming IPC result the citric acid/sodium chloride wash is repeated. Upon obtaining a conforming IPC for residual MR84910 content, the organic phase is concentrated under vacuum. Azeotropic distillation is then performed with additional 2-MeTHF (593 kg, 2.58 X) until the water content is not more than 0.5% w/w as measured by Karl Fischer analysis. In the event of a failing IPC result, an additional 2-MeTHF azeotropic distillation cycle is performed. The content of MR84915 in solution is then quantified by HPLC assay analysis to determine the amount of *p*-toluenesulfonic acid (*p*TSA) to be charged in the subsequent salt formation operation. To the MR84915 free base solution is then added acetone (911 kg, 3.96 X) followed by the partial addition of a solution of *p*TSA·H_2O (0.98 equiv.) in 2-MeTHF (198 kg,

0.86 X) to generate a seed bed. The resulting slurry is aged at 20–30°C and the remaining *p*TSA·H_2O/2-MeTHF solution is added. The mixture is then heated to 50–60°C and subsequently cooled to -15 to -5°C. The slurry is held at this temperature for 17 hours, and the solids are collected by filtration and the wet cake is washed with precooled acetone (308 kg, 1.34 X). The solids are then dried until the level of residual acetone is not more than 4000 ppm and the water content is not more than 0.5%. 263.4 kg of product was collected with potency of 98.9 wt% and 98.1% a/a purity (70% yield).

^{1}H NMR (400 MHz, DMSO-d_6) δ 9.65 (s, 1H), 7.96 – 7.89 (m, 1H), 7.75 (dd, *J* = 8.2, 3.6 Hz, 1H), 7.61 – 7.52 (m, 2H), 7.51 – 7.31 (m, 9H), 7.09 (d, *J* = 7.8 Hz, 2H), 5.06 – 5.23 (m, 2H), 4.64 – 4.52 (m, 2H), 4.49 – 4.39 (m, 1H), 4.21 (dd, *J* = 17.4, 8.7 Hz, 1H), 4.13 – 3.88 (m, 3H), 3.82 – 3.70 (m, 2H), 3.65 – 3.65 (m, 2H), 3.35 (br s, 3H), 3.21 – 2.83 (m, 9H), 2.26 (s, 3H), 2.26 – 2.17 (m, 1H), 2.10 – 1.98 (m, 1H), 1.96 – 1.75 (m, 2H) ppm. **^{13}C NMR** (101 MHz, DMSO-d_6) δ 166.0, 165.9, 164.5, 164.3, 161.2, 154.3, 154.2, 148.0, 147.8, 145.6, 137.7, 137.05, 137.0, 136.5, 129.6, 129.5, 128.8, 128.8, 128.6, 128.4, 128.1, 128.0, 127.6, 126.9, 126.9, 126.0, 125.5, 125.0, 124.9, 124.8, 124.8, 118.9, 118.6, 118.5, 109.3, 109.1, 66.8, 58.7, 58.5, 56.4, 50.0, 48.2, 47.3, 46.8, 26.2, 25.5, 25.2, 20.8, 18.2 ppm. Duplicates were observed for some signals due to atropisomerism. **HRMS** (ESI) calculated for $C_{37}H_{41}ClN_7O_3$: 666.2959 $[M+H]^+$, Found: 666.3036.

MR84916 (24): *N,N*-dimethylacetamide (DMAc) (717 kg, 2.81 X) and intermediate MR84915 Tosylate (255 kg, 1.00 X) to a suitable inert reaction vessel. To the vessel is then charged anhydrous K3PO4 (258 kg, 4.00 equiv.) which is rinsed into the mixture with additional DMAc (240 kg, 0.94 X). The reactor is degassed with nitrogen and to the vessel is then added 2-mercaptoethanol (48.5 kg, 0.19 X, 2.00 equiv.). The reaction mass is heated to a critical temperature range of 73–76°C and monitored by HPLC analysis. The conversion is considered to be complete when the level of residual MR84915 is not more than 0.4% a/a relative to product MR84916. Upon achieving a passing IPC result, the reaction stream is cooled to 25–30°C and to the vessel is charged purified water (638 kg, 2.50 X). The solution is warmed to approximately 35–45°C and held with agitation. The organic phase is separated and to it is then added purified water (179 kg, 0.70 X) while maintaining an internal temperature of 15–25°C. The mixture is seeded with intermediate MR84916, aged, and treated with additional purified water (459 kg 1.8 X) to complete crystallization. The solids are collected by filtration, washed with a mixture of purified water/DMAc (306 kg and 191 kg respectively; 1.2 X:0.75 X respectively), and the resulting wet solid is then slurried in a mixture of acetonitrile (58.7 kg, 0.23 X) and purified water (765 kg, 3.00 X). The product is then collected by filtration, washed twice with purified water (74 kg, 0.29 X) and subsequently dried under vacuum at not more than 40°C until the moisture content is NMT 10% by KF analysis. 157 kg of white solid was collected with potency of 93.5 wt% and 98.7% a/a purity (89% yield).

^{1}H NMR (400 MHz, DMSO-d_6) δ 7.90 (dd, *J* = 8.2, 1.3 Hz, 1H), 7.72 (d, *J* = 8.1 Hz, 1H), 7.56 (dd, *J* = 7.5, 1.3 Hz, 1H), 7.54 – 7.48 (m, 1H), 7.47 – 7.39 (m, 1H), 7.31 (dd, *J* = 7.4, 3.5 Hz, 1H), 4.24 (dd, *J* = 10.7, 4.8 Hz, 1H), 4.20 – 4.11 (m, 1H), 4.01 (ddd, *J* = 10.4, 6.5, 3.4 Hz, 1H), 3.92 – 3.78 (m, 1H), 3.76 – 3.64 (m, 2H), 3.51 – 3.41 (m, 1H), 3.16 – 2.98 (m, 3H), 2.98 – 2.86 (m, 3H), 2.86 – 2.55 (m, 6H), 2.49 – 2.43 (m, 1H), 2.31 (d, *J* = 1.5 Hz, 3H), 2.13 (q, *J* = 8.5 Hz, 1H), 1.97 – 1.83 (m, 1H), 1.72 – 1.50 (m, 3H) ppm. **^{13}C NMR** (101 MHz, DMSO-d_6) δ 165.8, 165.7, 163.9, 163.8, 162.1, 162.1, 148.1, 148.1, 137.0, 129.5, 128.9, 128.6, 126.9, 125.9, 124.9, 124.7, 118.8, 118.7, 108.4, 108.3, 68.8, 68.8, 63.4, 58.7, 58.6, 57.0, 57.0, 51.8, 51.7, 51.1, 50.7, 50.1, 50.0, 47.9, 47.6, 44.6, 41.3, 41.2, 28.6, 28.6, 25.7, 25.6, 22.5, 21.3, 21.1 ppm. Duplicates were observed for some signals due to atropisomerism. **HRMS** (ESI) calculated for $C_{29}H_{35}ClN_7O$: 532.2592 $[M+H]^+$, Found: 532.2706.

MRTX849 (1): The final step of MRTX849 drug substance manufacture begins by charging intermediate MR84916 (140 kg, 1.00X) and acetonitrile (1640 kg, 11.72 X) to a suitable inert reaction vessel. Azeotropic distillation is then performed with additional acetonitrile (1090 kg, 7.81 X) until the water content is not more than 0.3% w/w as measured by Karl Fischer analysis and the reaction volume is concentrated to 3.5 V. The concentrated MR84916 solution is then brought to 10–20°C and held. To a separate inerted reaction vessel is then charged acetonitrile (328 kg, 2.34 X) and MR84917-Na salt (50.4 kg, 0.36 X, 1.70 equiv.) at 10–20°C. The MR84917-Na salt solution is treated with a 50% w/w solution of T3P in ethyl acetate (251 kg, 1.79 X, 1.50 equiv.) while maintaining a temperature of 10-15°C and subsequently held at 14–18°C for not less than 2 hours. The MR84917 solution and the concentrated solution of MR84916 are combined while maintaining a batch temperature of 10–15°C. The reaction is held in this temperature range until the level of residual MR84916 is not more than 0.4% a/a relative to product MRTX849 by HPLC analysis. Upon achieving the end of reaction IPC criterion, the reaction mixture is basified with aqueous K_2CO_3 (11.9% w/w, 715 kg, 5.11 X) to give a mixture between pH 8–9. The organic phase is separated and washed with an aqueous solution of K_3PO_4 (20% w/w, 525 kg, 3.75 X) and the layers are separated. The organic solution is diluted with IPA (879 kg, 6.28 X) and treated with activated carbon. Solvent exchange to IPA is performed by cycles of concentration and addition of IPA under vacuum until the residual acetonitrile content is not more than 1.5% w/w. The batch is diluted with purified water (350 kg, 2.5 X). Following addition of MRTX849 seed, the batch is cooled, water added (350 kg, 2.5 X), and further cooled to 0–5°C.

The solids are collected by filtration and washed with a mixture of purified water (210 kg, 1.5 X) and IPA (34 kg, 0.24 X) followed by purified water (182 kg, 1.3 X), then re-slurried with purified water (182 kg, 1.3 X) until the pH of the filter cake is not more than 8.3. The crude MRTX849 is then dried under vacuum to a KF endpoint of not more than 1% w/w.

The crude MRTX849 (1.00 X, basis for recrystallization) is charged to a suitable reaction vessel and dissolved in IPA (6.28 X) at 58–60°C. The process stream is polish filtered into an inert crystallization vessel and to the resulting filtrate is added *n*-heptane (1.37 X) at 58–60°C. The solution is cooled to 43–47°C, seeded with MRTX849 Form 2 seed (0.015 X), then the resulting slurry is slowly cooled in stages to 20–25°C. The slurry is wet-milled at 20–25°C to achieve a D_{90} of not more than 150 µm. The milled slurry is cooled to 3–7°C, the product is collected by filtration and washed with a mixture of IPA (0.95 X) and *n*-heptane (0.54 X). After sweeping with nitrogen, the collected product is dried under vacuum at less than 40°C to achieve an acceptable volatiles content by GC analysis. The finished MRTX849 is de-lumped and sieved through a 30 mesh screen. 104.1 kg of white solid with 100.3 wt% assay and 99.95% a/a purity was obtained (70% yield).

^{1}H NMR (400 MHz, DMSO-d_6) δ 7.91 (dd, J = 8.2, 1.3 Hz, 1H), 7.57 (dt, J = 7.4, 1.1 Hz, 1H), 7.52 (q, J = 7.7 Hz, 1H), 7.43 (t, J = 7.8 Hz, 1H), 7.33 (ddd, J = 15.9, 7.6, 1.2 Hz, 1H), 5.38 (dd, J = 18.0, 4.1 Hz, 1H), 5.36 – 5.18 (m, 1H), 4.84 (s, 1H), 4.26 – 4.21 (m, 1H), 4.18 (dd, J = 16.1, 9.5 Hz, 1H), 4.08 – 3.94 (m, 2H), 3.91 – 3.86 (m, 1H), 3.75 (dd, J = 20.2, 17.4 Hz, 1H), 3.47 (q, J = 7.3 Hz, 1H), 3.23 (dd, J = 13.7, 3.7 Hz, 1H), 3.18 – 2.99 (m, 3H), 2.98 – 2.88 (m, 2H), 2.70 – 2.52 (m, 1H), 2.48 – 2.46 (m, 0H), 2.32 (d, J = 3.5 Hz, 3H), 2.14 (qd, J = 8.7, 2.2 Hz, 1H), 1.90 (dq, J = 12.1, 8.2 Hz, 1H), 1.71 – 1.50 (m, 3H) ppm. **^{13}C NMR** (101 MHz, DMSO-d_6) δ 165.9, 164.3 (d, J = 14.5 Hz), 162.1 (d, J = 2.1 Hz), 160.8 (dd, J = 31.7, 12.2 Hz), 155.6 (d, J = 266.7 Hz), 148.0 (d, J = 20.4 Hz), 137.0 (d, J = 2.9 Hz), 129.4 (d, J = 2.1 Hz), 128.9 (d, J = 4.3 Hz), 128.5, 126.8 (d, J = 2.6 Hz), 125.8, 125.0 (d, J = 5.6 Hz), 124.7 (d, J = 6.1 Hz), 118.7 (d, J = 2.6 Hz), 118.1 (d, J = 3.9 Hz), 108.7 (d, J = 20.7 Hz), 99.9 (d, J = 14.3 Hz), 68.9 (d, J = 7.0 Hz), 63.4 (d, J = 2.7 Hz), 58.5 (d, J = 25.8 Hz), 57.0 (d, J = 4.0 Hz), 50.0, 49.0, 48.2, 47.3 (d, J = 36.2 Hz), 46.4, 41.2 (d, J = 2.9 Hz), 28.5 (d, J = 7.1 Hz), 25.2 (d, J = 35.0 Hz), 22.5, 18.1 ppm. **^{19}F NMR** (376 MHz, DMSO-d_6) δ -105.18 (d, J = 334.7 Hz) ppm. **HRMS** (ESI) calculated for $C_{32}H_{36}ClFN_7O_2$: 604.2598 $[M+H]^+$, Found: 604.2607.

■ References

1. a) Punekar, S.R.; Velcheti, V.; Neel, B.G.; Wong, K.-K. The current state of the art and future trends in RAS-targeted cancer therapies. *Nat. Rev.,* **2022**, *19*, 637-655. b) Ledford, H. Closing in on cancer's deadliest mutations. *Nature*, **2022**, *610*, 620-622.
2. a) Hallin, J.; Engstrom, L.D.; Hargis, L.; Calinisan, A.; Aranda, R.; Briere, D.M.; Sudhakar, N.; Bowcut, V.; Baer, B.R.; Ballard, J.A.; Burkard, M.R.; Fell, J.B.; Fischer, J.P.; Vigers, G.P.; Xue, Y.; Gatto, S.; Fernandez-Banet, J.; Pavlicek, A. Velastagui, K.; Chao, R.C.; Barton, J.; Pierobon, M.; Baldelli, E.; Patricoin III, E.F.; Cassidy, D.P.; Marx, M.A.; Rybkin, I.I.; Johnson, M.L.; Ou, S.-H.I.; Lito, P.; Papadopoulos, K.P.; Jänne, P.A.; Olson, P.; Christensen, J.G. The KRAS^{G12C} inhibitor MRTX849 provides insight toward therapeutic susceptibility of KRAS-mutant cancers in mouse models and patients. *Cancer Discov.* **2020**, *10*, 54-71. b) Jänne, P.A.; Rybkin, I.I.; Spira, A.I.; Riely, G.J.; Papadopoulos, K.P.; Sabari, J.K.; Johnson, M.L.; Heist, R.S.; Bazhenova, L.; Barve, M.; Pacheco, J.M.; Leal, T.A.; Velastegui, K.; Cornelius, C.; Olson, P.; Christensen, J.G.; Kheoh, T.; Chao, R.C.; Ou, S.H.I. KRYSTAL-1: Activity and safety of adagrasib (MRTX849) in advanced/metastatic non-small-cell lung cancer (NSCLC) harboring KRAS G12C mutation. *Eur. J. Cancer,* **2020**, *138*, S1-S2. c) Ou, S.H.I.; Jänne, P.A.; Leal, T.A.; Rybkin, I.I.; Sabari, J.K.; Barve, M.A.; Bazhenova, L.; Johnson, M.L.; Velastegui, K.L.; Cilliers, C.; Christensen, J.G.; Yan, X.; Chao, R.C.; Papdopoulos, K.P. First-in-human Phase I/IB Dose-Finding Study of Adagrasib (MRTX849) in patients with advanced KRAS^{G12C} solid tumors (KRYSTAL-1). *J. Clin. Oncol.*, **2022**, *40*, 2530-2538.
3. Fell, J.B.; Fischer, J.P.; Baer, B.B.; Blake, J.F.; Bouhana, K.; Briere, D.M.; Brown, K.D.; Burgess, L.E.; Burns, A.C.; Burkard, M.R.; Chiang, H.; Chicarelli, M.J.; Cook, A.W.; Gaudino, J.J.; Hallin, J.; Hanson, L.; Hartley, D.P.; Hicken, E.J.; Hingorani, G.P.; Hinklin, R.J.; Mejia, M.J.; Olson, P.; Otten, J.N.; Rhodes, S.P.; Rodriguez, M.E.; Savechenkov, P.; Smith, D.J.; Sudhakar, N.; Sullivan, F.X.; Tang, T.P.; Vigers, G.P.; Wollenberg, L.; Christensen, J.G.; Marx, M.A. Identification of the clinical development candidate MRTX849, a covalent KRAS^{G12C} inhibitor for the treatment of cancer. *J. Med. Chem.*, **2020**, *63*, 6679-6693.
4. See supporting information for synthetic route to MR849109.
5. See supporting information for kinetics.
6. Olah, G. A.; Narang, S. C., Iodotrimethylsilane—a versatile synthetic reagent. *Tetrahedron* **1982**, *38*, 2225-2277.
7. Birkofer, L.; Bierwirth, E.; Ritter, A., Decarbobenzoxylierungen mit Triäthylsilan. *Chem. Ber.* **1961**, *94*, 821-824.
8. Scattolin, T.; Gharbaoui, T.; Chen, C.-y., A Nucleophilic Deprotection of Carbamate Mediated by 2-Mercaptoethanol. *Org. Lett.* **2022**, *24*, 3736-3740.
9. Older sample may develop a more unpleasant smell.

10. The work-up is described in the Experimental Section.